LETTER

https://doi.org/10.1038/s41586-018-0636-7

A mesocortical dopamine circuit enables the cultural transmission of vocal behaviour

Masashi Tanaka[1,5], Fangmiao Sun[2,3], Yulong Li[2,3,4] & Richard Mooney[1]*

The cultural transmission of behaviour depends on the ability of the pupil to identify and emulate an appropriate tutor[1–4]. How the brain of the pupil detects a suitable tutor and encodes the behaviour of the tutor is largely unknown. Juvenile zebra finches readily copy the songs of the adult tutors that they interact with, but not the songs that they listen to passively through a speaker[5,6], indicating that social cues generated by the tutor facilitate song imitation. Here we show that neurons in the midbrain periaqueductal grey of juvenile finches are selectively excited by a singing tutor and—by releasing dopamine in the cortical song nucleus HVC—help to encode the song representations of the tutor used for vocal copying. Blocking dopamine signalling in the HVC of the pupil during tutoring blocked copying, whereas pairing stimulation of periaqueductal grey terminals in the HVC with a song played through a speaker was sufficient to drive copying. Exposure to a singing tutor triggered the rapid emergence of responses to the tutor song in the HVC of the pupil and a rapid increase in the complexity of the song of the pupil, an early signature of song copying[7,8]. These findings reveal that a dopaminergic mesocortical circuit detects the presence of a tutor and helps to encode the performance of the tutor, facilitating the cultural transmission of vocal behaviour.

The cortical song nucleus HVC is crucial for singing and song learning[7,9–12] and receives convergent input from premotor, auditory and neuromodulatory neurons, including dopamine (DA)-secreting neurons in the midbrain periaqueductal grey (PAG)[13–15] (Fig. 1a–c and Extended Data Fig. 1a–c). In the mammalian PAG, DA neurons encode information about social context, arousal in response to behaviourally salient stimuli, or rewards[16–18], raising the possibility that the PAG-to-HVC pathway in juvenile finches encodes information about the tutor that facilitates song imitation. To explore this idea, we implanted tetrodes into the PAG of juvenile male finches raised in isolation from a tutor (tutor-naive juveniles; see Methods) (Fig. 1d–k). Most PAG neurons (81.8%; 18 out of 22 neurons from four birds) increased their action potential activity in the presence of a singing tutor (Fig. 1e–g, k), whereas PAG activity was unaffected during encounters with non-singing adult male finches or female finches, which do not sing (Fig. 1i–k). Neural activity in the PAG of the juvenile was not precisely locked to

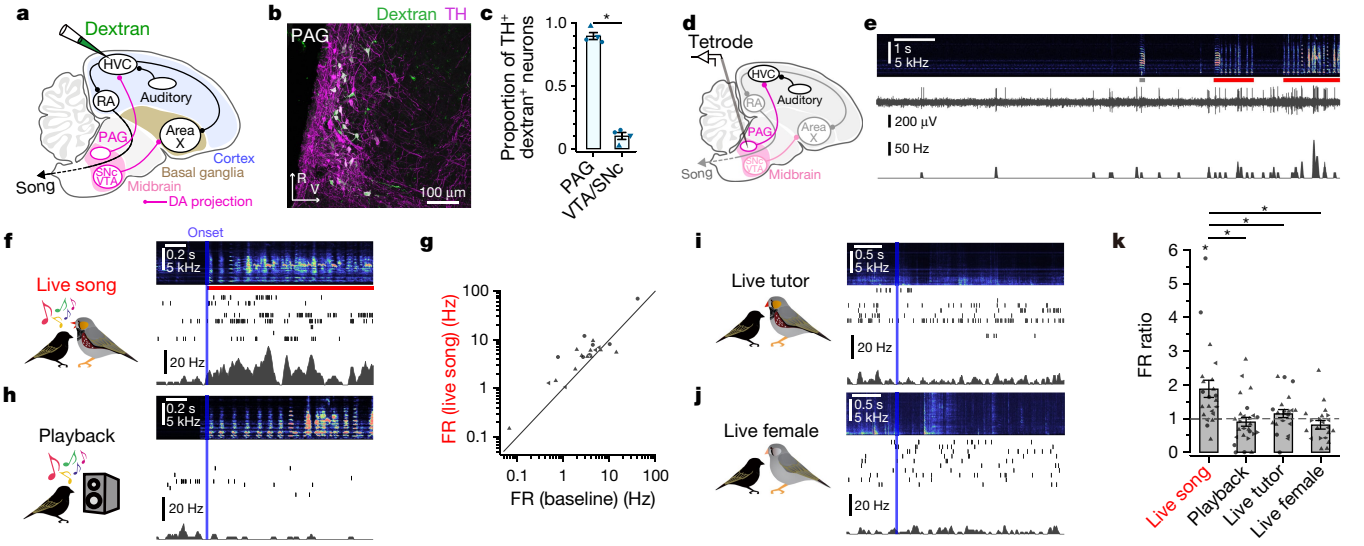

Fig. 1 | Recordings of PAG activity. a, Schematic of dextran injection into HVC. RA, robust nucleus of the arcopallium; SNc, substantia nigra pars compacta; VTA, ventral tegmental area. **b**, PAG neurons labelled with dextran (green) and TH antibody (pseudo-coloured magenta) (approximately 0.5 mm lateral of the midline). R, rostral; V, ventral. **c**, Proportion of double-labelled neurons (dextran and TH) in the midbrain. Data were analysed using a χ^2 test; $\chi_1^2 = 623.02$, $P < 0.001$, $n = 4$ hemispheres from three birds. **d**, Schematic of tetrode recordings from PAG neurons. **e**, PAG unit activity during live tutor songs (red bar) (grey bar: an isolated tutor call). Top, sound spectrogram. Middle, voltage recording. Bottom, firing rate. **f**, PAG unit activity aligned to the onset of tutor songs. Top, averaged spectrogram. Middle, spike raster. Bottom, mean firing rate. **g**, Mean firing rate (FR) during live tutor songs as a function of baseline firing rate of PAG neurons. **h**–**j**, PAG unit activity aligned to the onset of song playback (**h**), encounters with a live, non-singing tutor (**i**), encounters with a live female (**j**), shown as in **f**. **k**, Mean firing rate of PAG neurons normalized to baseline firing rate. Student's two-sided paired *t*-test, comparing firing rate during each condition to baseline; live song, $t_{21} = 3.439$, $P = 0.002$; playback, $t_{25} = 0.278$, $P = 0.783$; live tutor, $t_{21} = 1.270$, $P = 0.218$; live female, $t_{19} = 1.339$, $P = 0.196$; $n = 26$ neurons from five birds. Data are mean ± s.e.m. Asterisks above horizontal bars indicate significant *P* values from Tukey–Kramer tests in which the firing rate during live tutor songs is compared to other conditions: playback, $P < 0.001$; live tutor, $P = 0.017$; live female, $P < 0.001$.

[1]Department of Neurobiology, Duke University, Durham, NC, USA. [2]State Key Laboratory of Membrane Biology, Peking University School of Life Sciences, Beijing, China. [3]PKU-IDG/McGovern Institute for Brain Research, Beijing, China. [4]Peking-Tsinghua Center for Life Sciences, Beijing, China. [5]Graduate School of Life Sciences, Tohoku University, Sendai, Japan. *e-mail: mooney@neuro.duke.edu

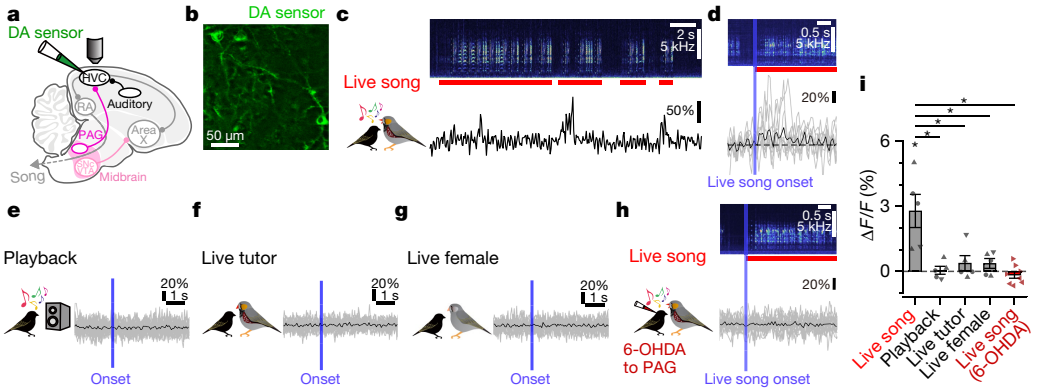

Fig. 2 | Imaging of DA in the HVC. a, Schematic of two-photon imaging of DA sensors ($GRAB_{DA1h}$) in the HVC. **b**, Two-photon image of HVC neurons expressing DA sensors. **c**, Fluorescence changes ($\Delta F/F$) of $GRAB_{DA1h}$ in a HVC neuron of a juvenile in response to songs from a live tutor (red bars). **d**, $\Delta F/F$ aligned to the onset of live tutor songs (grey, individual traces; black, mean). **e**–**h**, $\Delta F/F$ aligned to the onset of song playback (**e**), encounters with a live, non-singing tutor (**f**), encounters with a live female (**g**) and live tutor songs after 6-OHDA injection into the PAG (**h**). **i**, Mean $\Delta F/F$ of HVC neurons. Student's two-sided paired *t*-test; live song, $t_4 = 3.660$, $P = 0.022$; playback, $t_4 = 0.261$, $P = 0.807$; live tutor: $t_4 = 1.092$, $P = 0.336$; live female, $t_4 = 1.589$, $P = 0.187$; live song after 6-OHDA injection into the PAG, $t_7 = 1.122$, $P = 0.324$; $n = 13$ neurons from five birds. Data are mean ± s.e.m.

syllables of the song of the tutor, was variable across different tutor song bouts, and could remain elevated for hundreds of milliseconds after the tutor had stopped singing (Extended Data Fig. 2c–f), suggesting that PAG activity evoked by a singing tutor is not simply auditory in nature. Indeed, playback of the song of an adult finch from a speaker, including that of a recent tutor, failed to evoke activity in the PAG of the juvenile (Fig. 1h, k). Moreover, song playback from a speaker in the presence of an adult female bird failed to activate PAG neurons in tutor-naive juveniles (Extended Data Fig. 2a, b). Therefore, PAG neurons in juvenile males respond strongly and selectively to a live singing tutor and can thus signal the presence of a suitable song model.

These findings raise the possibility that experience of a singing tutor stimulates DA release from PAG terminals in the HVC. We explored this idea by virally expressing a modified dopamine type 2 (D2) receptor in HVC neurons of tutor-naive juvenile males that increases fluorescence upon DA binding (Fig. 2) (AAV2/9-$GRAB_{DA1h}$)[19]. We then head-fixed these juvenile males in the awake state and used two-photon imaging methods[20] to establish that DA levels in the HVC increase in the presence of a singing tutor (Fig. 2c–d, i). By contrast, DA-related changes in fluorescence were not detected in the HVC of the juvenile in response to song playback (Fig. 2e, i), or when the juvenile encountered non-singing adult males or females (Fig. 2f, g, i), paralleling the selective enhancement of PAG activity elicited by a singing tutor. Moreover, ablating DA neurons in the PAG of the pupil with 6-hydroxydopamine (6-OHDA[21]) prevented tutor-evoked DA transients in the HVC of the pupil (Fig. 2h, i), confirming that

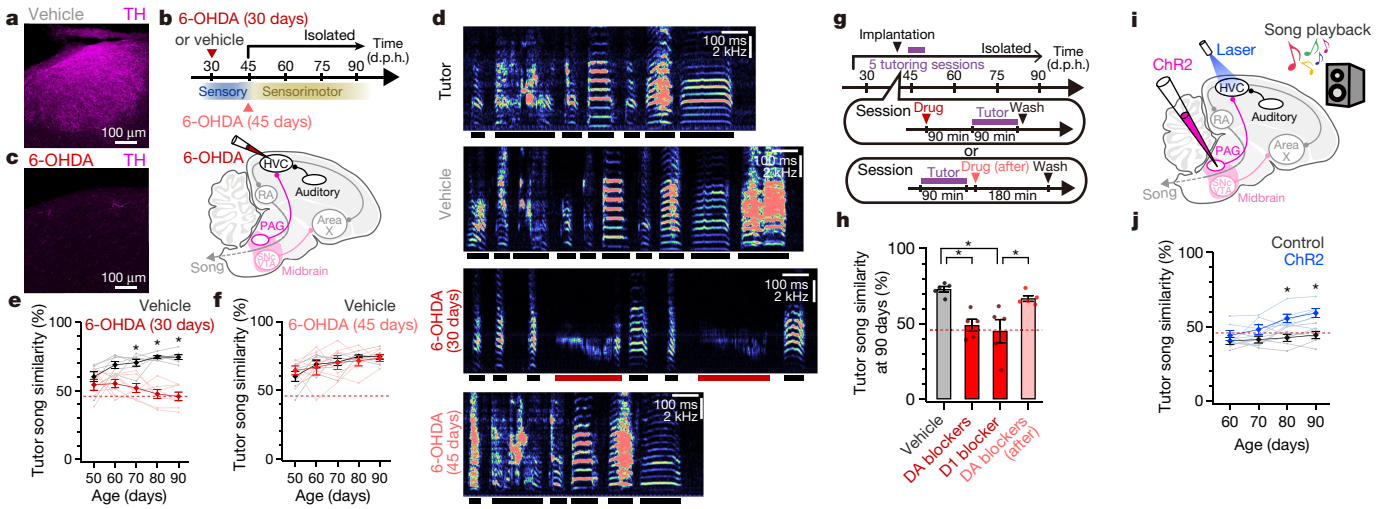

Fig. 3 | Chemical blockade and optogenetic activation of DA signalling in HVC. a, DA fibres in HVC (pseudo-coloured magenta, TH) (approximately 2.4 mm lateral of the midline). **b**, Timeline and schematic of 6-OHDA injection into the HVC. d.p.h., days after hatching. **c**, Loss of DA fibres in the HVC after 6-OHDA injection at 29 days of age, as in **a** (around 2.4 mm lateral of the midline). **d**, From top to bottom, spectrograms of a song from the tutor bird and songs from 90-day-old pupil birds that received injections into the HVC of vehicle, 6-OHDA at around 30 days of age or 6-OHDA at around 45 days of age (red bars denote abnormally long syllables; see Extended Data Fig. 4b, c). **e**, Absence of song copying following injection of 6-OHDA into the HVC at around 30 days of age. Tukey–Kramer test; vehicle, $n = 7$; 6-OHDA, $n = 7$; at 90 days, $P < 0.001$. **f**, Normal levels of song copying were achieved following injection of 6-OHDA into the HVC at around 45 days of age. Tukey–Kramer test; vehicle, $n = 7$ (same birds as in **e**); 6-OHDA at 45 days of age, $n = 6$; at 90 days, $P = 1.000$. **g**, Timeline of DA blocker infusion into the HVC using microdialysis. **h**, Tutor song similarity of 90-day-old pupils that received infusion into the HVC of vehicle during tutoring ($n = 5$), DA blockers during tutoring (Tukey–Kramer test; compared to vehicle, $P = 0.011$, $n = 5$), dopamine type 1(D1-type) receptor blocker during tutoring (Tukey–Kramer test; compared to vehicle, $P < 0.001$, $n = 5$), or DA blockers after tutoring (Tukey–Kramer test; compared to vehicle, $P = 1.000$; $n = 5$). **i**, Schematic of PAG_{HVC} terminal activation paired with song playback. **j**, Song copying is facilitated by pairing playback with PAG_{HVC} terminal activation in tutor-naive juveniles (Tukey–Kramer test; ChR2, $n = 6$; control, $n = 6$; at 90 days, $P = 0.023$). **e**, **f**, **h**, **j**, Horizontal red dashed lines show song similarity between 90-day-old untutored birds to unrelated adults (see Extended Data Fig. 4b, c). Data are mean ± s.e.m.

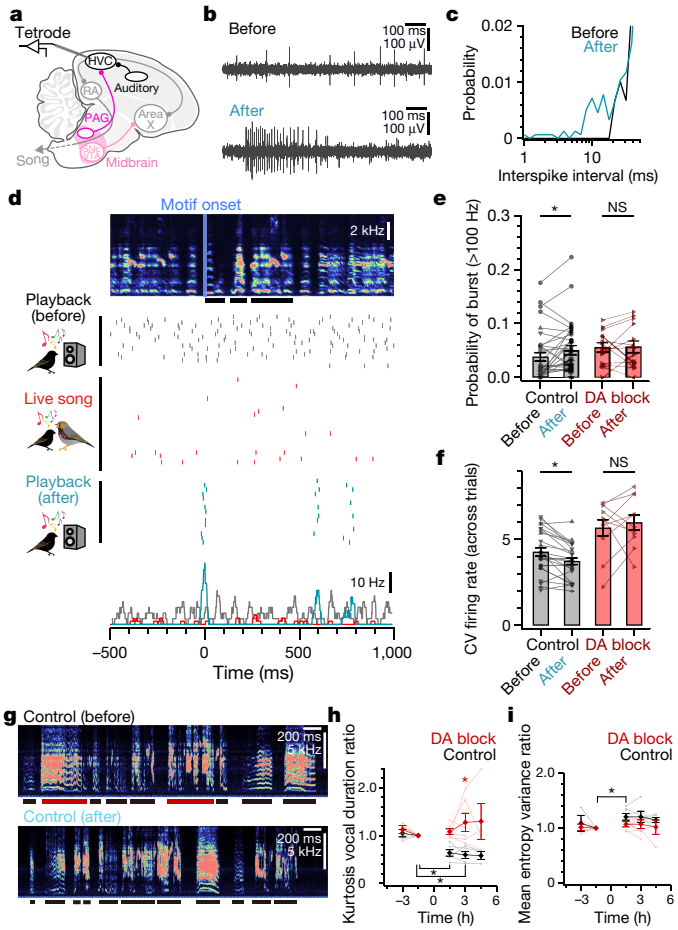

Fig. 4 | Changes in HVC activity and song features after live tutoring. **a**, Schematic of HVC recordings in pupils. **b**, **c**, Spontaneous HVC unit activity (**b**) and the histogram of the interspike intervals before (black) and after (cyan) live tutoring (**c**). **d**, HVC unit activity aligned to tutor song motif onset. Top, averaged spectrogram. Middle, raster. Bottom, mean firing rate across trials. Horizontal bars indicate syllables. **e**, Probability of burst activity (>100 Hz) increased after live tutoring in control juveniles (Student's two-sided paired *t*-test; $t_{34} = 2.490$, $P = 0.018$, $n = 35$ neurons from four birds), but not in juveniles with 6-OHDA injected into the HVC (Student's two-sided paired *t*-test; $t_{13} = 0.774$, $P = 0.453$, $n = 14$ neurons from two birds). NS, not significant. **f**, After live tutoring, coefficients of variance (CV) of firing rate across trials of tutor song playback decreased in control juveniles (Student's two-sided paired *t*-test; $t_{25} = 4.080$, $P < 0.001$, $n = 26$ neurons from four birds), but not in juveniles with 6-OHDA injected into the HVC (Student's two-sided paired *t*-test; $t_{10} = 0.640$, $P = 0.537$, $n = 11$ neurons from two birds). **g**, Spectrograms of juvenile songs before (top) and after (bottom) live tutoring (red bar: long vocalization). **h**, After live tutoring, kurtosis of vocal duration decreased in control juveniles (Student's two-sided paired *t*-test; 1.5 h, $t_5 = 5.563$, Bonferroni-corrected $P = 0.008$, $n = 6$), but not in juveniles with 6-OHDA or DA blockers injected into the HVC (Student's two-sided paired *t*-test; 1.5 h: $t_5 = 1.364$, Bonferroni-corrected $P = 0.692$, $n = 6$). **i**, After live tutoring, mean Wiener entropy variance increased in control juveniles (Student's two-sided paired *t*-test; at 1.5 h: $t_5 = 4.059$, Bonferroni-corrected $P = 0.029$, $n = 6$), but not in juveniles with 6-OHDA or DA blockers injected into HVC (Student's two-sided paired *t*-test; at 1.5 h: $t_5 = 1.432$, Bonferroni-corrected $P = 0.635$, $n = 6$). Juveniles did not sing during tutoring (0–1.5 h; see Extended Data Fig. 9). Data are mean ± s.e.m.

tutor-evoked DA release in the HVC of the pupil largely originates from the PAG.

To explore whether DA signalling in the HVC has a role in song imitation, we used 6-OHDA to lesion DA-releasing fibres in the HVC of juvenile male finches raised continuously with adult male tutors and tracked their song development into adulthood (Fig. 3a–c and Extended Data Fig. 3). Lesions of DA-releasing fibres in HVC made near the onset of the sensitive period for tutor song memorization (30 days after hatching[22]) prevented song copying (Fig. 3d, e) without affecting the overall rate of singing (Extended Data Fig. 4a). As adults, these 6-OHDA-treated birds produced abnormally long and acoustically simple syllables, similar to finches raised in isolation from a tutor[22] (Extended Data Fig. 4b, c). The 6-OHDA lesions made in the HVC in 30-day-old males are permanent and thus could potentially interfere with tutor song memorization (that is, sensory learning), the subsequent phase of song copying (sensorimotor learning), or both. However, 6-OHDA lesions made in the HVC of 45-day-old males, which have had sufficient tutoring experience to enable accurate copying but are just beginning sensorimotor learning[22], did not affect the ability of a juvenile to copy the song of a tutor (Fig. 3d, f).

These findings suggest that DA signalling in the HVC has a role in sensory learning, but we cannot exclude a more general but developmentally restricted (before 45 days of age, for example) role for such signalling. Therefore, we used microdialysis methods[23] to reversibly block DA receptors in the HVC[24] of tutor-naive juvenile males (age: 43.0 ± 4.9 days of age (mean ± s.d.), $n = 5$) while they were housed with a tutor for 1.5 h on five consecutive days, allowing us to better determine whether DA signalling in the HVC is crucial during pupil–tutor interactions, when sensory learning occurs (Fig. 3g, h and Extended Data Fig. 5a–c). Reversibly blocking DA receptors in the HVC during, but not immediately after, tutoring sessions blocked song copying (Fig. 3h and Extended Data Fig. 5b, c), without affecting attentive behaviours of juveniles to tutors or the singing rates of tutors (Extended Data Fig. 5d, e and Supplementary Videos 1, 2). Moreover, reversibly suppressing PAG activity in the pupil with muscimol during daily tutoring sessions also blocked song copying; notably, juveniles in which the PAG was inactivated also failed to orient to their tutors, even though tutors continued singing at normal rates (Extended Data Fig. 5d–h and Supplementary Video 3). Thus, tutor-evoked activation of the PAG of the pupil and concomitant release of DA in the HVC are essential to encoding tutor song experience, and PAG activity may be required for the pupil to attend to a singing tutor.

The current findings do not exclude the possibility that DA signalling at other sites also contributes to sensory learning. One potential site is the basal ganglia region, Area X[11], which receives dopaminergic input from the ventral tegmental area and substantia nigra pars compacta, as well as from a smaller cohort of TH^+ PAG neurons (Extended Data Fig. 1d–g), and where dopamine signalling has a role in sensorimotor learning[25]. Nevertheless, infusing DA receptor blockers into Area X of juvenile males during daily tutoring sessions did not affect song copying (Extended Data Fig. 6). Another potential site is the caudal mesopallium, an auditory forebrain region important for song memory[26,27]. However, blocking DA receptors in the caudal mesopallium of juvenile males during daily tutoring sessions did not block song copying (Extended Data Fig. 5i–k).

These results show that DA release from PAG axon terminals in the HVC (PAG_{HVC} terminals) signals the presence of a suitable model and helps to encode this model in the brain of the pupil. Consequently, artificially activating PAG_{HVC} terminals should compensate for the absence of a live tutor and facilitate vocal copying in response to song playback. To test this hypothesis, we used adeno-associated viruses (AAVs) to express channelrhodopsin-2 (ChR2) bilaterally in the PAG of tutor-naive juvenile males (Fig. 3i, j and Extended Data Fig. 7a–d). Several weeks (33.3 ± 7.4 days (mean ± s.d.), $n = 6$) later, we implanted optical fibres bilaterally over the HVC and optogenetically activated PAG_{HVC} terminals while playing the song of an adult male zebra finch through a speaker. Pairing PAG_{HVC} terminal stimulation with song playback resulted in a significant level of song copying compared to juveniles that had only been exposed to song playback, or to song playback and optical illumination of HVC in the absence of ChR2 (Fig. 3j and Extended Data Fig. 7b; see Methods). Moreover, the combination of song playback and PAG_{HVC} terminal stimulation while infusing DA blockers into the HVC did not lead to song copying in tutor-naive juveniles (Extended Data Fig. 7e–g).

To explore how tutor-evoked DA release from PAG_{HVC} axon terminals alters HVC to drive song imitation, we implanted tetrodes in

the HVC of tutor-naive juveniles and recorded neural activity before and after their initial encounters with a singing tutor (Fig. 4a–f). Spontaneous burst firing in HVC neurons increased within 1 h after the initial exposure of the juvenile to a singing tutor (Fig. 4b, c, e), without any change in their mean firing rates (Extended Data Fig. 8d). Because burst firing in HVC is driven by auditory afferent neurons[12], this enhanced burst firing suggests that tutoring rapidly potentiates auditory inputs to the HVC. In fact, brief (35.0 ± 16.8 min (mean $\pm$ s.d.)) experience with a singing tutor led rapidly (around 1 h) to the emergence of temporally precise responses in the HVC of an awake juvenile to tutor song playback (Fig. 4d, f and Extended Data Fig. 8a–c). Furthermore, the mean firing rate of HVC neurons to song playback was unaffected by tutoring (Extended Data Fig. 8e, f), indicating that neural responses in the HVC became more tightly locked to specific features in the tutor song. None of these juveniles ($n = 4$) sang during or for several hours after the tutoring session, and thus these physiological changes were not simply the result of auditory feedback associated with vocal rehearsal. In another set of tutor-naive juvenile males, we found that tutoring rapidly reduced the kurtosis of vocal duration (Fig. 4g, h) and increased the mean entropy variance of the songs of the juveniles (Fig. 4i), two early hallmarks of song copying[7,8]. Notably, blocking DA signalling in the HVC of the pupil with 6-OHDA or DA blockers prevented these physiological and behavioural changes (Fig. 4e, f, h, i).

The discovery that DA neurons in the PAG of the pupil are strongly and selectively activated by a singing tutor parallels emerging evidence that potentially homologous neurons in the mammal can encode social cues, including those related to reward, context or novelty[16,17]. Indeed, the present findings advance a model in which both social cues and the song-related auditory input provided by the singing tutor drive the coincident activation of DA receptors and auditory synapses in the HVC, leading to the rapid emergence of auditory representations of the song of the tutor necessary to song imitation[10,20] (Extended Data Fig. 10). This coincident encoding mechanism could help to ensure that the brain of the pupil selectively forms representations of songs produced by suitable adult tutors, and not of extraneous auditory stimuli. Although DA-dependent modulation of auditory cortical representations has previously been linked to perceptual learning[28], a notable feature of the DA-dependent process of auditory encoding described here is that it occurs in a vocal motor region and rapidly drives vocal imitation. More broadly, DA signalling is enhanced in the motor cortex of primates relative to other mammals[29,30], raising the possibility that augmented DA signalling in motor regions of songbirds and primates reflects a convergent neural architecture for promoting motor imitation in response to social models.

Online content

Any methods, additional references, Nature Research reporting summaries, source data, statements of data availability and associated accession codes are available at https://doi.org/10.1038/s41586-018-0636-7.

Received: 30 March 2018; Accepted: 21 August 2018;
Published online: 17 October 2018

1. Whiten, A. Social learning and culture in child and chimpanzee. *Annu. Rev. Psychol.* **68**, 129–154 (2017).
2. Goldstein, M. H., King, A. P. & West, M. J. Social interaction shapes babbling: testing parallels between birdsong and speech. *Proc. Natl Acad. Sci. USA* **100**, 8030–8035 (2003).
3. Marler, P. & Tamura, M. Culturally transmitted patterns of vocal behavior in sparrows. *Science* **146**, 1483–1486 (1964).
4. Fehér, O., Wang, H., Saar, S., Mitra, P. P. & Tchernichovski, O. De novo establishment of wild-type song culture in the zebra finch. *Nature* **459**, 564–568 (2009).
5. Chen, Y., Matheson, L. E. & Sakata, J. T. Mechanisms underlying the social enhancement of vocal learning in songbirds. *Proc. Natl Acad. Sci. USA* **113**, 6641–6646 (2016).
6. Derégnaucourt, S., Poirier, C., Kant, A. V., Linden, A. V. & Gahr, M. Comparisons of different methods to train a young zebra finch (*Taeniopygia guttata*) to learn a song. *J. Physiol. Paris* **107**, 210–218 (2013).
7. Aronov, D., Andalman, A. S. & Fee, M. S. A specialized forebrain circuit for vocal babbling in the juvenile songbird. *Science* **320**, 630–634 (2008).
8. Derégnaucourt, S., Mitra, P. P., Fehér, O., Pytte, C. & Tchernichovski, O. How sleep affects the developmental learning of bird song. *Nature* **433**, 710–716 (2005).
9. Nottebohm, F., Stokes, T. M. & Leonard, C. M. Central control of song in the canary, *Serinus canarius*. *J. Comp. Neurol.* **165**, 457–486 (1976).
10. Roberts, T. F., Gobes, S. M., Murugan, M., Ölveczky, B. P. & Mooney, R. Motor circuits are required to encode a sensory model for imitative learning. *Nat. Neurosci.* **15**, 1454–1459 (2012).
11. Fortune, E. S. & Margoliash, D. Parallel pathways and convergence onto HVc and adjacent neostriatum of adult zebra finches (*Taeniopygia guttata*). *J. Comp. Neurol.* **360**, 413–441 (1995).
12. Coleman, M. J. & Mooney, R. Synaptic transformations underlying highly selective auditory representations of learned birdsong. *J. Neurosci.* **24**, 7251–7265 (2004).
13. Appeltants, D., Absil, P., Balthazart, J. & Ball, G. F. Identification of the origin of catecholaminergic inputs to HVc in canaries by retrograde tract tracing combined with tyrosine hydroxylase immunocytochemistry. *J. Chem. Neuroanat.* **18**, 117–133 (2000).
14. Hamaguchi, K. & Mooney, R. Recurrent interactions between the input and output of a songbird cortico-basal ganglia pathway are implicated in vocal sequence variability. *J. Neurosci.* **32**, 11671–11687 (2012).
15. Kingsbury, M. A., Kelly, A. M., Schrock, S. E. & Goodson, J. L. Mammal-like organization of the avian midbrain central gray and a reappraisal of the intercollicular nucleus. *PLoS ONE* **6**, e20720 (2011).
16. Cho, J. R. et al. Dorsal raphe dopamine neurons modulate arousal and promote wakefulness by salient stimuli. *Neuron* **94**, 1205–1219 (2017).
17. Matthews, G. A. et al. Dorsal raphe dopamine neurons represent the experience of social isolation. *Cell* **164**, 617–631 (2016).
18. Flores, J. A., Galan-Rodriguez, B., Ramiro-Fuentes, S. & Fernandez-Espejo, E. Role for dopamine neurons of the rostral linear nucleus and periaqueductal gray in the rewarding and sensitizing properties of heroin. *Neuropsychopharmacology* **31**, 1475–1488 (2006).
19. Sun, F. et al. A genetically encoded fluorescent sensor enables rapid and specific detection of dopamine in flies, fish, and mice. *Cell* **174**, 481–496 (2018).
20. Roberts, T. F., Tschida, K. A., Klein, M. E. & Mooney, R. Rapid spine stabilization and synaptic enhancement at the onset of behavioural learning. *Nature* **463**, 948–952 (2010).
21. Ungerstedt, U. & Arbuthnott, G. W. Quantitative recording of rotational behavior in rats after 6-hydroxy-dopamine lesions of the nigrostriatal dopamine system. *Brain Res.* **24**, 485–493 (1970).
22. Eales, L. A. Song learning in zebra finches: some effects of song model availability on what is learnt and when. *Anim. Behav.* **33**, 1293–1300 (1985).
23. Tanaka, M., Singh Alvarado, J., Murugan, M. & Mooney, R. Focal expression of mutant huntingtin in the songbird basal ganglia disrupts cortico-basal ganglia networks and vocal sequences. *Proc. Natl Acad. Sci. USA* **113**, E1720–E1727 (2016).
24. Kubikova, L., Wada, K. & Jarvis, E. D. Dopamine receptors in a songbird brain. *J. Comp. Neurol.* **518**, 741–769 (2010).
25. Hisey, E., Kearney, M. G. & Mooney, R. A common neural circuit mechanism for internally guided and externally reinforced forms of motor learning. *Nat. Neurosci.* **21**, 589–597 (2018).
26. Roberts, T. F. et al. Identification of a motor-to-auditory pathway important for vocal learning. *Nat. Neurosci.* **20**, 978–986 (2017).
27. London, S. E. & Clayton, D. F. Functional identification of sensory mechanisms required for developmental song learning. *Nat. Neurosci.* **11**, 579–586 (2008).
28. Bao, S., Chan, V. T. & Merzenich, M. M. Cortical remodelling induced by activity of ventral tegmental dopamine neurons. *Nature* **412**, 79–83 (2001).
29. Berger, B., Gaspar, P. & Verney, C. Dopaminergic innervation of the cerebral cortex: unexpected differences between rodents and primates. *Trends Neurosci.* **14**, 21–27 (1991).
30. Williams, S. M. & Goldman-Rakic, P. S. Widespread origin of the primate mesofrontal dopamine system. *Cereb. Cortex* **8**, 321–345 (1998).

Acknowledgements We thank J. Hatfield for constructing AAV2/9-CAG-GRAB$_{DA1h}$; S. Nowicki, S. Peters, C. Sturdy, F. Wang and S. Soderling for critical discussion and for reading earlier versions of this manuscript. This work was supported by JSPS Postdoctoral Fellowship for Research Abroad (M.T.), the National Basic Research Program of China 973 Program Grant 2015CB856402 (Y.L.), the American BRAIN Initiative project 1U01NS103558-01 (Y.L.), NIH Grant 1R01-NS-099288 (R.M.) and NSF IOS-1354962 (R.M.).

Reviewer information *Nature* thanks O. Tchernichovski, L. Zweifel and the other anonymous reviewer(s) for their contribution to the peer review of this work.

Author contributions M.T. and R.M. designed experiments. F.S. and Y.L. developed DA sensors. M.T. performed experiments and analysed data. M.T. and R.M. wrote the manuscript.

Competing interests F.S. and Y.L. have filed patent applications of which the value might be affected by this publication.

Additional information
Extended data is available for this paper at https://doi.org/10.1038/s41586-018-0636-7.
Supplementary information is available for this paper at https://doi.org/10.1038/s41586-018-0636-7.
Reprints and permissions information is available at http://www.nature.com/reprints.
Correspondence and requests for materials should be addressed to R.M.
Publisher's note: Springer Nature remains neutral with regard to jurisdictional claims in published maps and institutional affiliations.

METHODS

Data reporting. No statistical methods were used to predetermine sample size. The experiments were not randomized and the investigators were not blinded to allocation during experiments and outcome assessment.

Animal model. Juvenile male (15–90 days old), adult male (>200 days old) and adult female (>200 days old) zebra finches (*Taeniopygia guttata*) were obtained from the Duke University Medical Center breeding facility. All experimental procedures were in accordance with the NIH guidelines and approved by the Duke University Medical Center Animal Care and Use Committee. Birds were kept under a 14:10-h light:dark cycle with free access to food and water. Data were collected from 96 birds (Supplementary Table).

Song analysis. Songs were automatically recorded with Sound Analysis Pro (SAP2011)[31] in a soundproof box. Vocalizations of >10 ms were detected by thresholding of the recorded sounds. Imitation of the tutor song was quantified as percentage of similarity (asymmetrical similarity) between the song motifs from pupil birds and their tutors using SAP2011[31] with default parameters for zebra finches, and reported as tutor song similarity. First, the song motif (a stereotyped sequence of syllables constituting an adult zebra finch song) of each bird was determined as the most frequently observed syllable sequence. Then, the percentage of similarity was calculated for representative song motifs randomly chosen from pupils and their tutor, and averaged across ≥10 comparisons to report as tutor song similarity. For immature subsongs that do not have a stereotyped song motif, we used a randomly chosen part of the subsongs with a duration that was similar to the tutor song motif for calculating the percentage of similarity. For isolated birds in Extended Data Fig. 4c, the percentage of similarity was calculated between the song motifs from isolated birds and unrelated, normally raised adult zebra finches. A song bout was detected as successive vocalizations with ≥3 syllables (to exclude call bouts) separated by an interbout interval of >400 ms. Kurtosis of vocal duration and Wiener entropy variance were calculated based on all of the song bouts in each 90-min time window.

Tutoring of juvenile birds. Juvenile birds were raised by their parents with their siblings until around 45 days old in experiments depicted in Fig. 3a–f. Otherwise, juvenile birds were separated from their parents and siblings at 15–30 days of age (that is, tutor-naive juveniles), and encountered an unfamiliar adult male (tutor) only during tutoring sessions. During a tutoring session, a juvenile bird and tutor were separated by a plastic grating or transparent glass, so they could acoustically and visually interact but direct physical interactions were prevented. The tutor was either manually introduced into the neighbouring chamber by an experimenter, or presented through an electric glass for which the transparency could be remotely controlled. Attention of juvenile birds to the tutor was quantified as the time that juvenile birds were awake and near the tutor without foraging, drinking, preening or singing, and normalized to the total time of observation (>5 min) during tutoring sessions. Untutored isolated birds depicted in Extended Data Fig. 4b, c were kept isolated from adult males until 90 days of age.

General surgery. Detailed procedures of surgery were previously provided[23]. In brief, juvenile birds were anaesthetized with 2% isoflurane inhalation and placed on a custom stereotaxic apparatus with a heat blanket. Target cites for injection and implantation were determined by stereotaxic coordinates and multiunit activity. Stereotaxic coordinates, measured from the bifurcation of the midsagittal sinus, were 0.0 mm rostral, 2.4 mm lateral and 0.5 mm ventral for HVC; 3.4 mm rostral, 0.5 mm lateral and 6.3 mm ventral (head angle of 58°) for PAG; 5.8 mm rostral, 1.6 mm lateral and 3.0 mm ventral (head angle of 40°) for Area X; and 1.3 mm rostral, 1.2 mm lateral and 0.5 mm ventral for the caudal mesopallium (CM). Reagents or viruses were injected using Nanoject-II (Drummond Scientific). Viral injections were performed bilaterally with a volume of 483–966 nl per hemisphere. Viruses were obtained from the Penn Vector Core (Pennsylvania, USA), UNC Vector Core (Chapel Hill, USA), Janelia Virus Service Facility (Ashburn, USA), and Vigene Biosciences (Rockville, USA). Experiments were performed >30 days after the viral injection. Birds with unsuccessful injection or implantation were discarded from the analysis.

Injection of 6-OHDA. Juvenile birds received bilateral injection of 200–450 nl 6-OHDA solution into the HVC at either around 30 days of age (mean ± s.d.: 30.1 ± 4.2 days of age; range: 25–34 days of age; $n = 7$) or around 45 days of age (mean ± s.d.: 44.5 ± 3.0 days of age; range: 39–47 days of age; $n = 6$). The solution was PBS-based and included 5–20 mM 6-OHDA hydrochloride (Santa Cruz, sc-203482), 2–10 mM L-ascorbic acid (Millipore/Sigma, A92902), and 1 μM desipramine hydrochloride (Tocris, 3067), which was included as an inhibitor for noradrenaline and serotonin transporters to protect noradrenergic and serotonergic neuron terminals at the injection site. Control birds received an injection of PBS with 2–10 mM ascorbic acid and 1 μM desipramine at around 30 days of age (mean ± s.d.: 29.3 ± 3.6 days of age; range: 22–32 days of age; $n = 7$). Drugs were dissolved into PBS immediately before injection in place of equimolar NaCl (working solution: around 300 mOsm, pH 7.3). After injection, birds were returned to their original home cage until approximately 45 days of age when they were isolated in a soundproof box until 90 days of age.

Microdialysis infusion of drugs. Tutor-naive juveniles (around 45 days of age; mean ± s.d.: 43.8 ± 5.5 days of age; range: 32–57 days of age; $n = 34$) received bilateral implantation of a microdialysis probe. After 1–3 days of implantation (mean ± s.d.: 45.5 ± 5.8 days of age; range: 33–60 days of age; $n = 34$), tutoring sessions were conducted for five consecutive days. Each tutoring session consisted of 90-min tutor presentation. Drug was infused into the target area (HVC, Area X, CM or PAG) either 90 min before or immediately after the tutor presentation, and washed with saline 180 min after the injection (Fig. 3g). The tutor bird typically sang >30 motifs in a session (see Extended Data Fig. 5e). For a session in which the tutor did not sing any song, an additional tutoring session was conducted on the next day. As a blocker for D1- and D2-type receptors, 5 mM R(+)-SCH-23390 hydrochloride (Millipore/Sigma, D054) and 5 mM S-(−)-sulpiride (Tocris, 0895) were respectively used and dissolved into saline. To inactivate PAG, 2.5 mM muscimol (Millipore/Sigma, M-1523) dissolved into saline was infused into the PAG.

Histology and imaging. Birds were deeply anaesthetized with intramuscular injection of 20 μl euthasol (Virbac) and transcardially perfused with PBS, followed by perfusion with 4% (wt/vol) paraformaldehyde (PFA) in PBS. The removed brain was post-fixed and cryoprotected with 30% (wt/vol) sucrose and 4% (wt/vol) PFA in PBS overnight. Frozen sagittal sections (thickness of 50 μm) were prepared with a sledge microtome (Reichert) and collected in PBS. For immunohistochemistry, sections were washed twice in PBS, permeabilized with 0.3% Triton X-100 in PBS (PBST) for 1 h, blocked with 10% Blocking One Histo (06349-64, Nacalai Tesque) in PBST for 1 h, and incubated with rabbit primary antibody against TH (1:500, AB152; Millipore/Sigma) or rabbit primary antibody against dopamine beta-hydroxylase (DBH) (1:2,000, 22806; ImmunoStar) in PBST with 10% Blocking One Histo at 4 °C overnight. Then, sections were washed three times in PBST and incubated with anti-rabbit secondary antibody (1:500; Jackson ImmunoResearch) in PBST at room temperature for 1 h, followed by three washes in PBS. Sections were coverslipped with Fluoromount-G (SouthernBiotech), and then imaged with a confocal microscope (SP8; Leica) through a 20× objective lens controlled by LAS X software (Leica). To label PAG neurons that project to the HVC or Area X, dextran Alexa Fluor 488 (D-22910; ThermoFisher) was injected into the HVC (age: mean ± s.d.: 35.3 ± 7.0 days of age; range: 28–42 days of age; $n = 3$) or Area X (age: mean ± sd: 47.7 ± 15.3 days of age; range: 36–65 days of age; $n = 3$) of juvenile birds 4–7 days before perfusion. Retrogradely labelled neurons were manually counted in PAG and VTA/SNc, each of which was densely packed with TH^+ neurons. Images are shown as maximum-projected images of sagittal sections. To quantify TH^+ fibres in the HVC, TH^+ fibres in HVC shelf/nidopallium caudolateral (NCL), and DBH^+ fibres in the HVC, the fibre density was calculated in >0.04 mm^2 areas from each region as the fraction of areas with fluorescence higher than mean + 10 s.d. of the background fluorescence. For analysis of HVC shelf/NCL, a >0.04 mm^2 region located approximately 0.6 mm ventral of the HVC was manually selected.

Two-photon imaging and analysis. Viruses encoding DA sensors (AAV2/9-hSyn-$GRAB_{DA1h}$ or AAV2/9-CAG-$GRAB_{DA1h}$), developed in the Y.L. laboratory[19], were injected into the HVC of tutor-naive juveniles (approximately 30 days old, mean ± s.d.: 32.6 ± 5.3 days of age; range: 25–39 days of age; $n = 5$), and the HVC was imaged after implantation of a head-post and cranial window >30 days later (mean ± s.d.: 66.6 ± 6.0 days of age; range: 60–73 days of age; $n = 5$). To ablate DA-releasing PAG neurons, 200 nl 6-OHDA solution (10 mM 6-OHDA, 10 mM L-ascorbic acid, and 1 μM desipramine hydrochloride) was injected into PAG two days before imaging. Images were collected at 15.5 Hz with a resonant-scanning two-photon microscope (Neurolabware) that applies a mode-locked titanium sapphire laser (Mai Tai DeepSee) at 920 nm through a 16× objective lens (0.8 NA water immersion, Nikon). The objective lens was covered with black cloth to prevent room light from being detected by the photomultipliers. During imaging, a head-fixed bird in a dim room experienced playback of an adult zebra finch (tutor) song bout (3 s; seven introductory notes and three motifs comprising five syllables), encounters with an adult male tutor, encounters with an adult female bird, and a singing tutor with a randomized order. Images were acquired >10 trials for each condition, and regions of interest (ROIs) were automatically or manually selected after image alignment with MATLAB programs (Scanbox). After subtraction of background fluorescence in an annular region surrounding each ROI, signals were calculated as mean fluorescence within each ROI. Then, the $\Delta F/F$ of the ROI (%) was calculated for each trial as $100 \times (F(t) - F_0)/F_0$, where $F(t)$ was a time series of ROI signals, and F_0 was the average of baseline ROI signals for the 5-s period just before the onset of stimulus presentation. Mean $\Delta F/F$ was calculated for the 5-s period after the onset of stimulus presentation, and averaged across trials in each condition.

Optogenetics. Tutor-naive juvenile birds received an injection of AAV2/9-CAG-ChR2-mCherry, AAV2/1-CAG-ChR2-mCherry or AAV2/9-CAG-NRX-ChR2-YFP into the PAG at around 35 days of age (mean ± s.d.: 34.0 ± 4.8 days of age; range: 30–40 days of age; $n = 9$). A laser was bilaterally applied through optic fibres (core: 200 μm; Thorlabs) implanted into the HVC. Juvenile birds received a tutoring session

per day for five consecutive days starting at around 60–70 days of age (mean ± s.d.: 64.0 ± 4.9 days of age; range: 61–71 days of age; $n = 9$). In each tutoring session, a juvenile bird experienced playback of a song bout (mean amplitude: 70 dB sound pressure level, seven introductory notes and three motifs comprising five syllables) 10 times (30 motifs) within 30 min. To block DA signalling in the HVC, DA blockers were infused into the HVC with microdialysis probes 90 min before the tutoring session, and washed with saline immediately after the tutoring session ($n = 3$). Experimental birds received repetitive laser stimulation (10 ms; 20 Hz) throughout the playback. Control birds consisted of a group that received an injection of viruses encoding GFP and implantation of optic fibres ($n = 2$, scAAV2/9-CMV-GFP or AAV2/9-CAG-GFP) at around 35 days of age (mean ± s.d.: 36.5 ± 6.4 days of age; range: 32–41 days of age; $n = 2$), a group that did not receive viral injection but implantation of optic fibres ($n = 2$), and a group that did not receive injection, implantation or laser stimulation ($n = 2$). These groups listened to playback in the same way as experimental birds (age: mean ± s.d.: 58.5 ± 8.5 days of age; range: 54–73 days of age; $n = 6$), and were analysed together since we did not find any significant differences in learning abilities between these groups.

Chronic recording from the PAG and HVC. Tetrodes (A2x2-tet-3/10mm-150-150-121, NeuroNexus) were implanted into the HVC or the PAG of tutor-naive juveniles (age: mean ± s.d.: 51.3 ± 13.4 days of age; range: 27–71 days of age; $n = 11$). Birds were habituated to a dummy probe (1.5–2 g) on the head for approximately seven days before the implantation. Data were collected with a universal serial bus (USB) interface board (RHD2000; Intan Technologies) after band-pass filtering (0.2–10 kHz) and sampling at 30 kHz with a small amplifier board (RHD2132 16-Channel; Intan Technologies) on the head of the bird. Unit activity was sorted in a semi-automated fashion with custom C++ software using a support vector machine algorithm (M.T.). Unit activity with a mean amplitude >3 s.d. of noise was used for subsequent analyses. Recording of song-related activity was triggered by xpctarget in MATLAB (MathWorks). To block DA signalling in the HVC, juvenile birds received an injection of 6-OHDA into the HVC 2–5 days before tetrode recording from the same HVC. The mean firing rate of PAG neurons was calculated for >10 trials with >0.5 s after the onset of singing or song playback and 5 s after presentation of a male or female bird, and averaged after normalization with mean spontaneous firing rate calculated for >10 s before the presentation of stimuli. Probability of burst activity in HVC neurons was calculated for >300 s spontaneous activity before and after exposure to a live tutor. Coefficients of variance of the firing rate across trials of HVC neurons were calculated for 50-ms bins with a hop size 1 ms across >15 trials, and reported as the mean of the coefficients of variance of the firing rate from all the bins in the motif (>0.5 s) if the mean firing rate during playback was >0.05 Hz. For data analysis, Igor Pro (WaveMetrics), MATLAB and Microsoft Excel were used.

Statistics. Data are shown as mean ± s.e.m., unless otherwise noted. Two-way ANOVAs were performed in MATLAB to examine the significance of the main effect of 6-OHDA ($F_{2,85} = 53.10$, $P < 0.001$; Fig. 3e–f), DA blockers on the HVC, DA blockers on the CM and muscimol on PAG ($F_{5,99} = 23.17$, $P < 0.001$; Fig. 3h and Extended Data Fig. 5c, h, k), DA blockers on Area X ($F_{1,30} = 0.22$, $P = 0.640$; Extended Data Fig. 6c), optogenetic activation of PAG terminals in the HVC ($F_{2,47} = 16.61$, $P < 0.001$; Fig. 3j and Extended Data Fig. 7f), followed by a post hoc Tukey–Kramer test to report significant differences between conditions at each age window. To examine the different proportion of labelled neurons in the PAG and VTA/SNc, χ^2 tests were performed. Two-way ANOVAs were performed in MATLAB to examine significance of the main effect of blockage of DA signalling on kurtosis syllable duration ($F_{1,39} = 19.69$, $P < 0.001$; Fig. 4h), entropy variance ($F_{1,39} = 4.84$, $P = 0.034$; Fig. 4i) and song rate ($F_{1,39} = 0.16$, $P = 0.691$; Extended Data Fig. 9), followed by a Tukey–Kramer test to report significant differences between conditions at each time window and by a Student's two-sided paired t-test with Bonferroni correction to report significant differences between before and after exposure to tutor songs. One-way ANOVAs were performed in MATLAB to examine the main effect of different conditions in Fig. 1k and Extended Data Fig. 2b ($F_{4,93} = 6.84$, $P < 0.001$), Fig. 2i ($F_{4,23} = 10.31$, $P < 0.001$), Extended Data Fig. 3c ($F_{2,12} = 13.42$, $P < 0.001$), Extended Data Fig. 3d ($F_{2,12} = 0.14$, $P = 0.870$), Extended Data Fig. 4a ($F_{2,17} = 0.28$, $P = 0.757$), Extended Data Fig. 5d ($F_{2,7} = 30.40$, $P < 0.001$), and Extended Data Fig. 5e ($F_{2,10} = 0.78$, $P = 0.486$), each followed by a Tukey–Kramer test to report significant differences between conditions. In other analyses, Student's paired t-tests (Figs. 1k, 2i, 4h, i and Extended Data Figs. 2b, 8d–f) or Student's unpaired t-tests (Extended Data Figs. 3e, 4c) were performed in Microsoft Excel. Multiple data from a bird are indicated with the same markers in Fig. 1c, g, k, 2i, 4e, f and Extended Data Figs. 1b, c, e–g, 2b, 3c–e, 8d–f. Statistical tests were performed two-sided. Asterisks show $P < 0.050$.

Reporting summary. Further information on research design is available in the Nature Research Reporting Summary linked to this paper.

Code availability. Custom code or software is available from the corresponding author upon reasonable request.

Data availability

The datasets generated and analysed during the current study are available from the corresponding author upon reasonable request.

31. Tchernichovski, O., Nottebohm, F., Ho, C. E., Pesaran, B. & Mitra, P. P. A procedure for an automated measurement of song similarity. *Anim. Behav.* **59**, 1167–1176 (2000).

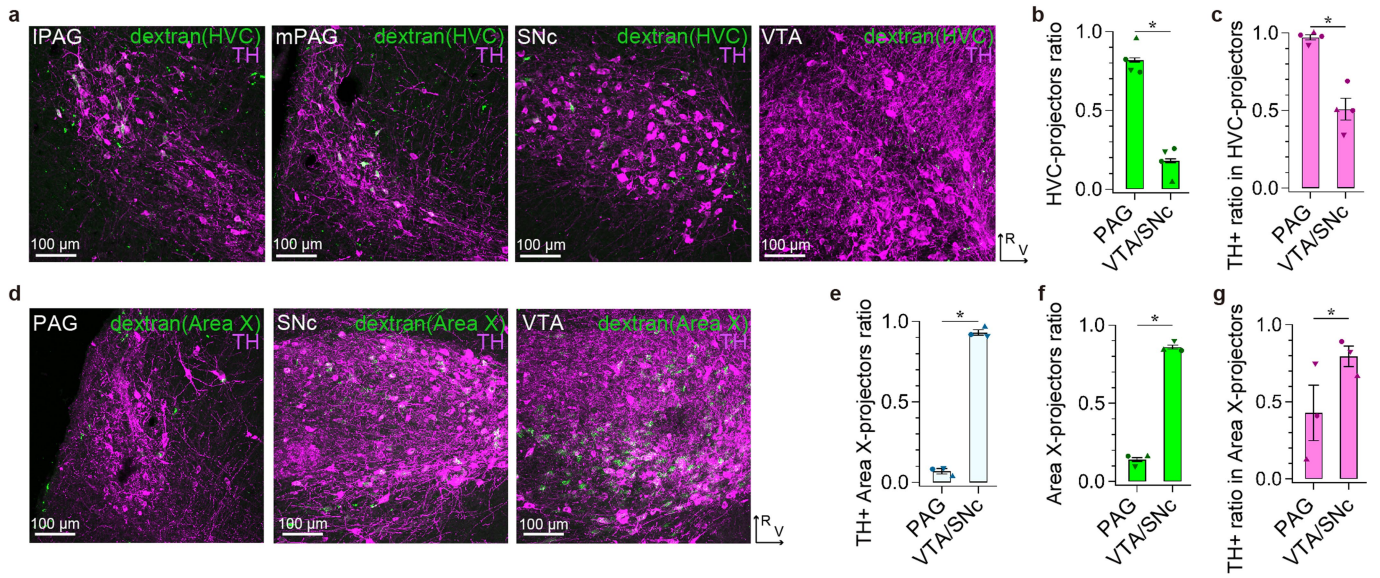

Extended Data Fig. 1 | Distribution of HVC-projecting neurons and Area X-projecting neurons in the midbrain. a, From left to right, a maximum-projected image of serial sagittal sections visualized with a confocal microscope, showing a lateral part of the PAG (lPAG) (approximately 1.0 mm lateral of the midline), a medial part of the PAG (mPAG, approximately 0.2 mm lateral of the midline), SNc (approximately 1.2 mm lateral of the midline) and VTA (approximately 0.2 mm lateral of the midline), each of which was labelled with dextran injected into the HVC (green) and an antibody against TH (pseudo-coloured magenta). Similar results were obtained in four independently repeated experiments. R, rostral; V, ventral. **b**, Proportion of HVC-projecting neurons in the PAG and VTA/SNc. χ^2 test; $\chi_1^2 = 406.54$, $P < 0.001$, $n = 4$ hemispheres from three birds. **c**, Proportion of TH^+ neurons in HVC-projecting neuron subsets in the PAG and the VTA/SNc. χ^2 test; $\chi_1^2 = 204.62$, $P < 0.001$, $n = 4$ hemispheres from three birds. **d**, From left to right, a maximum-projected image of serial sagittal sections visualized with a confocal microscope, showing the PAG (approximately 0.6 mm lateral of the midline), SNc (approximately 0.6 mm lateral of the midline) and VTA (approximately 0.2 mm lateral), each of which was labelled with dextran injected into Area X (green) and an antibody against TH (pseudo-coloured magenta). Similar results were obtained in three independently repeated experiments. **e**, Proportion of double-labelled neurons (dextran and TH) in PAG and SNc/VTA in birds that received injection of dextran into Area X. χ^2 test; $\chi_1^2 = 493.92$, $P < 0.001$, $n = 3$ hemispheres from three birds. **f**, Proportion of Area-X-projecting neurons in the PAG and VTA/SNc. χ^2 test; $\chi_1^2 = 472.07$, $P < 0.001$, $n = 3$ hemispheres from three birds. **g**, Proportion of TH^+ neurons in Area-X-projecting neuron subsets in the PAG and VTA/SNc. χ^2 test; $\chi_1^2 = 55.14$, $P < 0.001$, $n = 3$ hemispheres from three birds. Data are mean ± s.e.m.

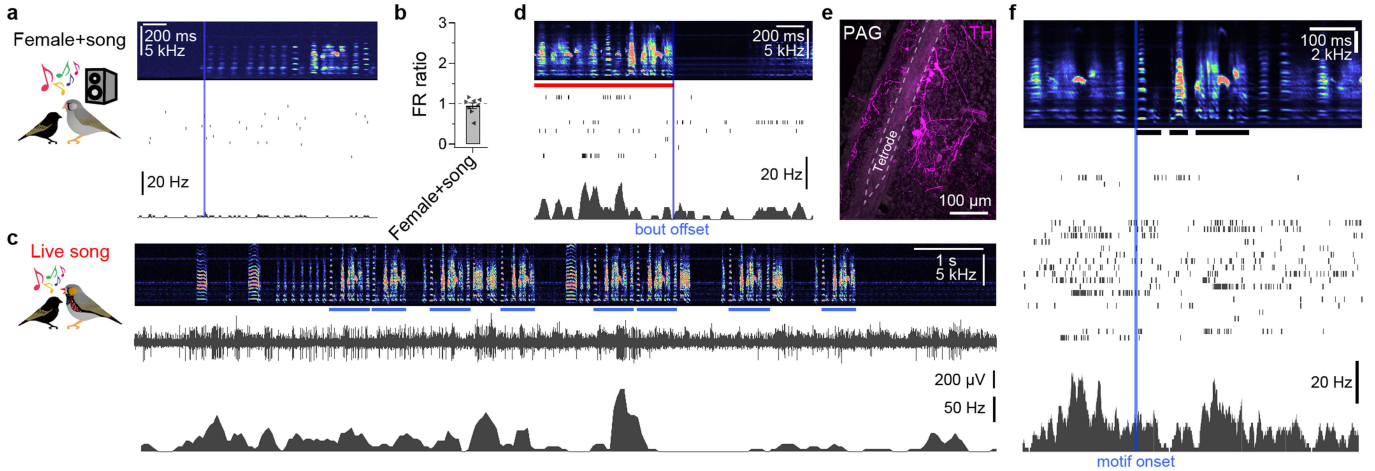

Extended Data Fig. 2 | Juvenile male PAG activity in response to song playback in the presence of a female bird and live songs of a male bird. **a**, Tutor-naive juvenile male finch PAG activity aligned to the onset of 35 presentations of song playback in the presence of an adult female bird. Top, averaged sound spectrogram. Middle, spike raster plot. Bottom, mean firing rate. Blue vertical bar marks song onset. **b**, Mean firing rate of neurons in the juvenile PAG during presentation of song playback in the presence of an adult female bird, normalized to baseline firing rate. Student's two-sided paired *t*-test; $t_7 = 0.620$, $P = 0.555$; $n = 8$ neurons from two birds. **c**, Neuron activity in the PAG of the juvenile during a live tutor song bout. Top, sound spectrogram. Middle, voltage recording. Bottom, firing rate. Blue bar, song motif. **d**, Juvenile PAG unit activity aligned to the offset (blue vertical bar) of the song bouts of a live tutor (red bar, live song), shown as in **a**. **e**, A maximum-projected image of serial sagittal sections visualized with a confocal microscope, showing the site of tetrode recordings in the PAG (around 0.8 mm lateral of the midline). **f**, Juvenile PAG unit activity aligned to the onset (blue vertical bar) of the song motifs (syllables denoted by black horizontal bars) of a live tutor, shown as in **a**. Note that the tutor often sings multiple motifs within a single bout, thus some motifs precede (and follow) the alignment time. Data are mean ± s.e.m.

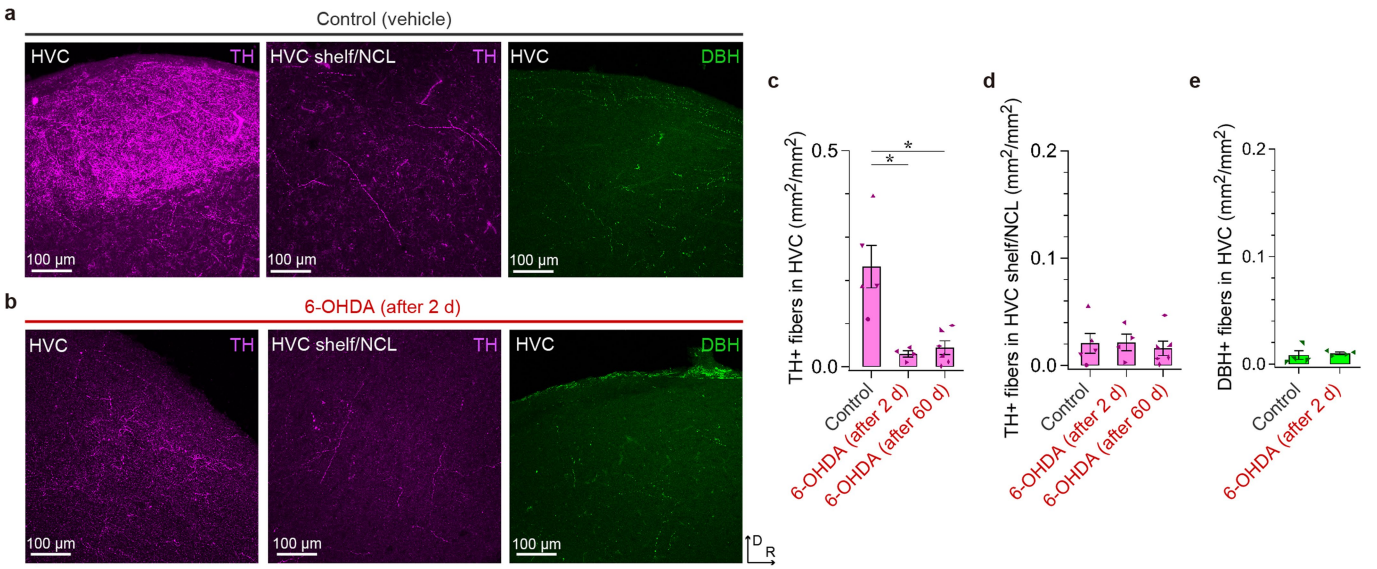

Extended Data Fig. 3 | Effects of 6-OHDA injection into the HVC on DA fibres in the HVC and surrounding regions and on noradrenergic/adrenergic fibres in the HVC. a, From left to right, a maximum-projected image of serial sagittal sections visualized with a confocal microscope, showing the HVC with TH immunolabelling (approximately 2.4 mm lateral of the midline), the HVC shelf and nidopallium caudolateral (NCL) just ventral of the HVC with TH immunolabelling (approximately 2.4 mm lateral of the midline), and the HVC with DBH immunolabelling (approximately 2.4 mm lateral of the midline) in control birds, which received an injection of vehicle into the HVC. Similar results were obtained in five independently repeated experiments (orientation is similar to **b**). **b**, From left to right, a maximum-projected image of serial sagittal sections visualized with a confocal microscope, showing the HVC with TH immunolabelling (approximately 2.4 mm lateral of the midline), the HVC shelf and NCL just ventral to the HVC with TH immunolabelling (approximately 2.4 mm lateral of the midline), and the HVC with DBH immunolabelling (approximately 2.4 mm lateral of the midline) in birds that received an injection of 6-OHDA into the HVC two days before tissue fixation. Similar results were obtained in four independently repeated experiments. D, dorsal; R, rostral. **c**, Density of TH^+ fibres in the HVC of control birds ($n = 5$ hemispheres from three birds) was higher than the density in birds that received injections of 6-OHDA two days before fixation (Tukey–Kramer test; $P = 0.002$; $n = 4$ hemispheres from two birds), and also higher than the density in birds that received injections of 6-OHDA around 60 days before fixation, as in Fig. 3b, c (Tukey–Kramer test; $P = 0.002$; $n = 6$ hemispheres from four birds). **d**, Density of TH^+ fibres in the HVC shelf and NCL in control birds ($n = 5$ hemispheres from three birds), birds that received an injection of 6-OHDA two days before fixation ($n = 4$ hemispheres from two birds), and birds that received an injection of 6-OHDA around 60 days before fixation, as in Fig. 3b, c ($n = 6$ hemispheres from four birds). **e**, Density of DBH^+ fibres in HVC in control birds ($n = 4$ hemispheres from two birds) and birds that received an injection of 6-OHDA two days before injection ($n = 4$ hemispheres from two birds) was not significantly different. Student's two-sided unpaired t-test; $t_7 = 0.379$, $P = 0.716$. Data are mean ± s.e.m.

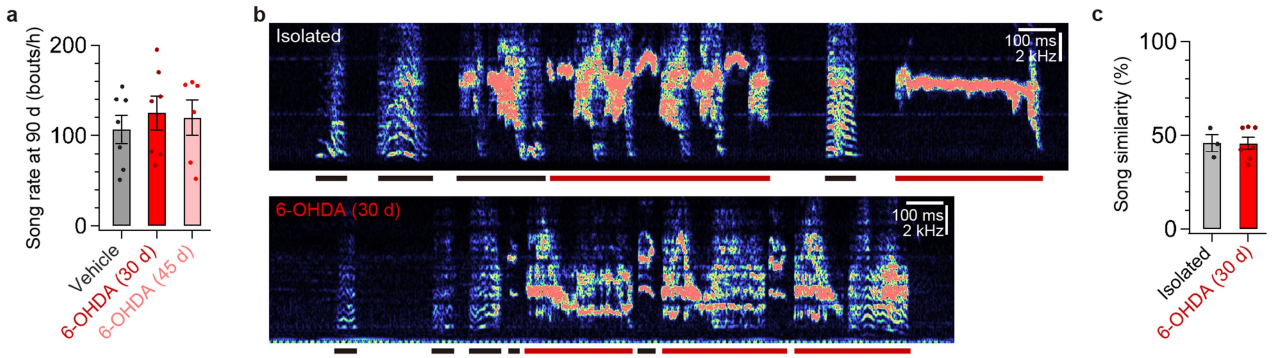

Extended Data Fig. 4 | Ablation of DA terminals in the HVC did not affect song rate but decreased song imitation to the level of birds raised in isolation from a tutor. a, The song rates of 90-day-old birds that received an injection of vehicle ($n = 7$), 6-OHDA at around 30 days of age ($n = 7$), and 6-OHDA at around 45 days of age ($n = 6$) were not significantly different. One-way ANOVA; $F_{2,17} = 0.283$, $P = 0.757$. **b**, Spectrograms from a 90-day-old bird that was raised in isolation from a tutor (top) and from a 90-day-old bird that was normally tutored but received an injection of 6-OHDA into the HVC at 30 days of age (bottom). **c**, Similarity of 90-day-old untutored (Isolated) adult zebra finch songs to songs of unrelated adult zebra finches that had been normally tutored ($n = 3$) was not significantly different from tutor song similarity of 90-day-old pupils that received an injection of 6-OHDA into the HVC at approximately 30 days of age ($n = 7$; Student's two-sided unpaired t-test; $t_9 = 0.013$, $P = 0.990$), but was significantly different from tutor song similarity of 90-day-old pupils that received an injection of vehicle at around 30 days of age ($n = 7$; Student's two-sided unpaired t-test; $t_9 = 3.028$, $P = 0.014$), or from tutor song similarity of 90-day-old pupils that received an injection of 6-OHDA into the HVC at around 45 days of age ($n = 6$; Student's two-sided unpaired t-test; $t_8 = 3.314$, $P = 0.011$). The song data from birds injected with 6-OHDA into the HVC at around 30 days of age is the same as in Fig. 3e; song similarity data from birds injected into the HVC with vehicle at around 30 days of age or 6-OHDA at around 45 days of age are not shown here but are shown in Fig. 3f. Data are mean ± s.e.m.

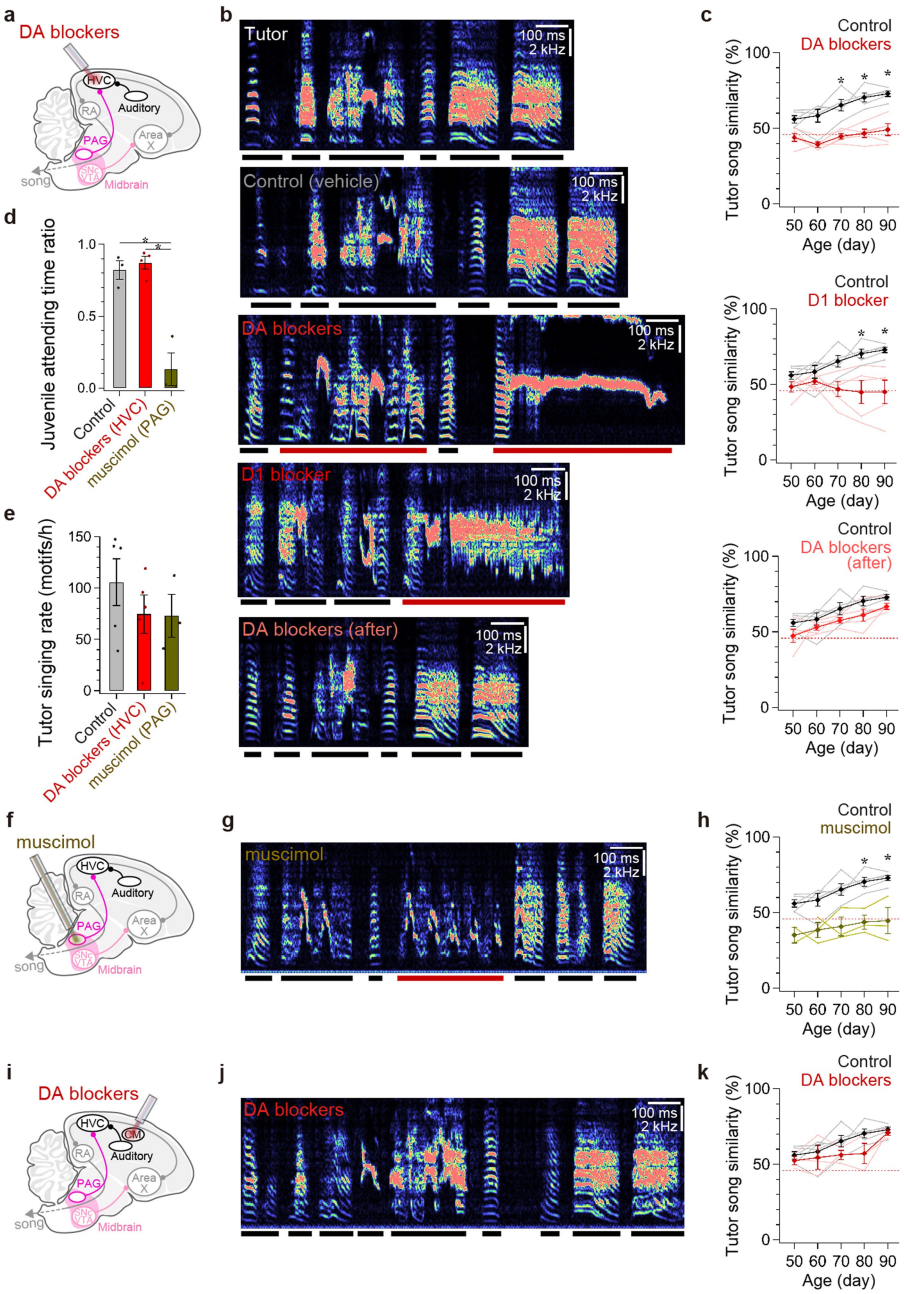

Extended Data Fig. 5 | See next page for caption.

Extended Data Fig. 5 | Effects of infusing DA blockers into either the HVC or CM, or infusing muscimol into the PAG on song copying. **a**, Schematic showing infusion of DA blockers into the HVC. **b**, From top to bottom, sound spectrograms of a song of a tutor bird, a 90-day-old pupil that received an infusion of vehicle during tutoring sessions, a 90-day-old pupil that received infusions of both D1- and D2-type DA blockers (DA blockers) during tutoring sessions, a 90-day-old pupil bird that received an infusion of a D1-type blocker during tutoring sessions, and a 90-day-old pupil that received infusions of both D1- and D2-type DA blockers after tutoring sessions. **c**, Developmental changes in tutor song similarity of pupils that received infusions of both D1- and D2-type DA blockers (DA blockers) into the HVC during tutoring sessions (top, $n = 5$), a D1-type blocker into HVC during tutoring sessions (middle, $n = 5$), or DA blockers into the HVC immediately after tutoring sessions (bottom, $n = 5$). Asterisks indicate $P < 0.050$; Tukey–Kramer test (see Methods). **d**, Proportion of time that juvenile birds attended to the tutor during tutoring sessions was not significantly different between birds that received infusions of vehicle ($n = 3$) or DA blockers into HVC ($n = 4$) (Tukey–Kramer test; $P = 0.871$). By contrast, the attention time of juvenile birds that received infusion of muscimol into the PAG ($n = 3$) was lower than that of control birds (Tukey–Kramer test; $P = 0.001$) and that of birds that received an injection of DA blockers into the HVC (Tukey–Kramer test; $P < 0.001$). **e**, Singing rates of the tutor bird to pupils that received vehicle into the HVC ($n = 5$) were not differe*n*t from that to pupils that received injection of DA blockers into the HVC ($n = 5$) or muscimol into the PAG ($n = 3$). One-way ANOVA; $F_{2,10} = 0.776$, $P = 0.486$. **f**, Schematic showing infusion of muscimol into the PAG. **g**, A sound spectrogram of a song of a 90-day-old pupil that received an infusion of muscimol into the PAG during tutoring sessions. A sound spectrogram of the tutor song is shown in **b**. **h**, Tutor song similarity of pupil birds that received infusion of vehicle into the HVC and birds that received an infusion of muscimol blockers into PAG were significantly different (Tukey–Kramer test; vehicle, $n = 5$; muscimol into the PAG, $n = 3$; at 90 days of age, $P = 0.007$). **i**, Schematic showing infusion of DA blockers into the CM (DA blockers possibly diffused into both the medial and lateral CM). **j**, A sound spectrogram of a song of a 90-day-old pupil that received an infusion of DA blockers into the CM during tutoring sessions. A sound spectrogram of the tutor song is shown in **b**. **k**, Tutor song similarity of pupil birds that received an infusion of vehicle into the HVC and birds that received infusion of DA blockers into the CM were not significantly different (Tukey–Kramer test; vehicle, $n = 5$; DA blockers into the CM, $n = 3$; at 90 days of age; $P = 1.000$). **c**, **h**, **k**, Horizontal red dashed lines show song similarity between 90-day-old untutored birds and unrelated adult male zebra finches that had been raised with normal exposure to a tutor (see Extended Data Fig. 4b, c). Data are mean ± s.e.m.

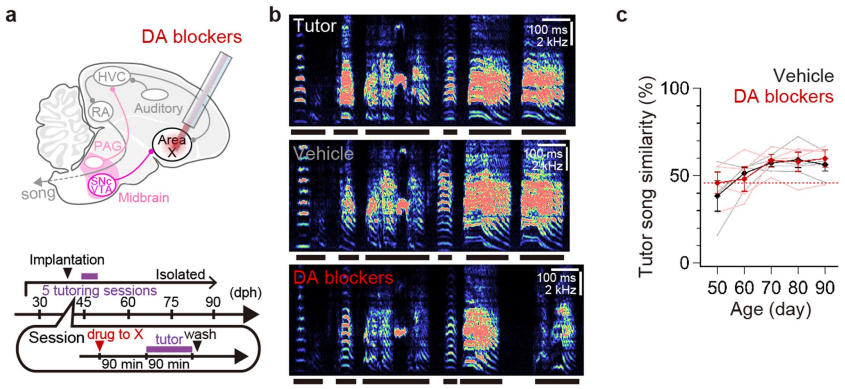

Extended Data Fig. 6 | Infusion of DA blockers into Area X in juvenile males did not disrupt song copying. a, Schematic (top) and schedule (bottom) of infusion of DA blockers into Area X. **b**, Sound spectrograms of a song of a tutor (top), a 90-day-old bird that received an infusion of vehicle into Area X during tutoring sessions (middle), and a 90-day-old bird that received an infusion of DA blockers into Area X during tutoring sessions (bottom). **c**, Tutor song similarity of pupil birds that received an infusion of vehicle into Area X and birds that received infusion of DA blockers into Area X were not significantly different. Tukey–Kramer test; vehicle, $n = 4$, DA blockers, $n = 4$; at 90 days of age; $P = 1.000$. The horizontal red dashed line shows song similarity between 90-day-old untutored birds and unrelated adult male zebra finches that had been raised with normal exposure to a tutor (see Extended Data Fig. 4b, c). Data are mean ± s.e.m.

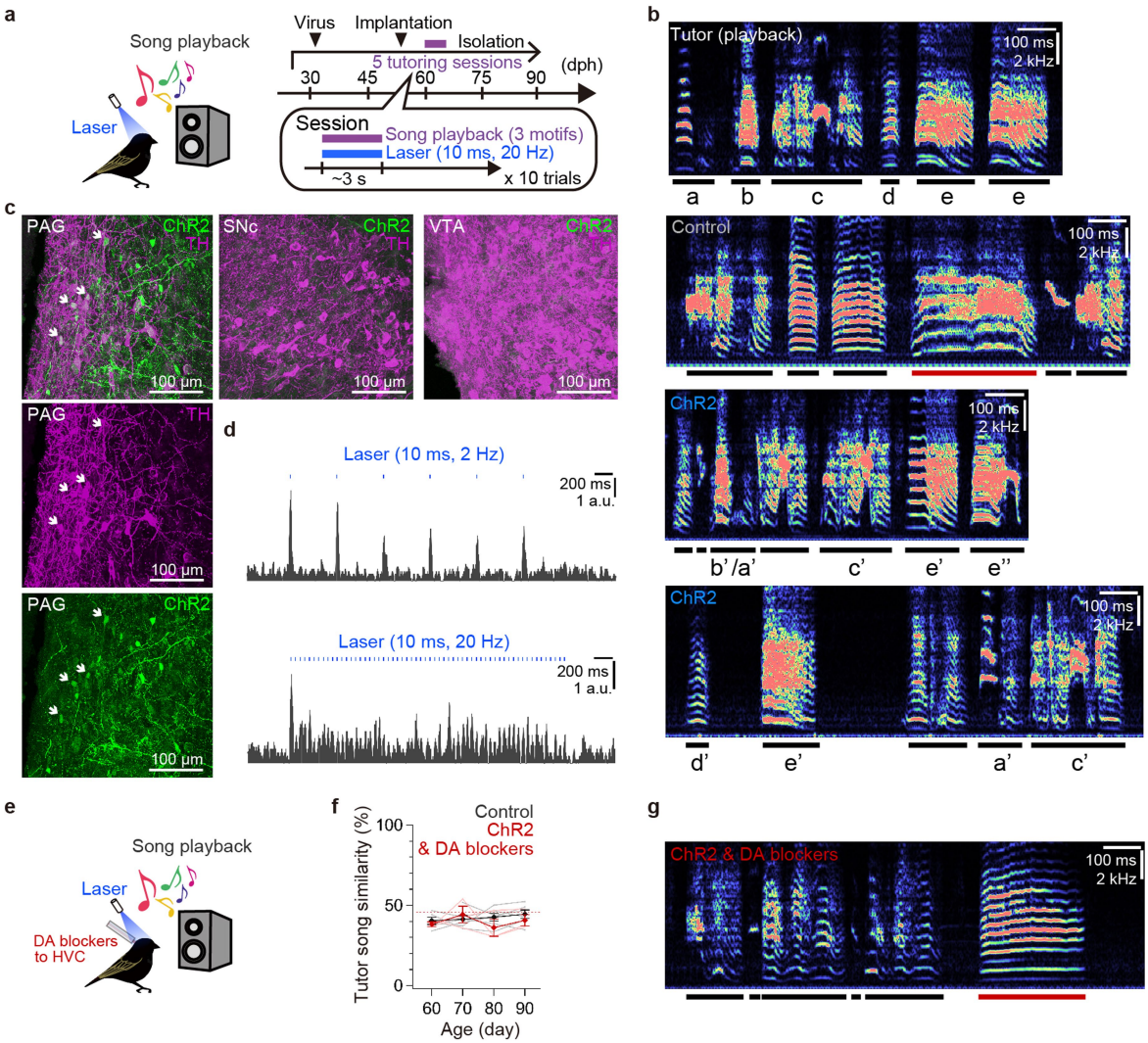

Extended Data Fig. 7 | Optogenetic activation of PAG_{HVC} terminals paired with song playback. a, Schematic (left) and schedule (right) of optogenetic stimulation of PAG_{HVC} terminals paired with song playback. **b**, Sound spectrograms of song playback used in tutoring sessions (top), a song of a 90-d pupil 'tutored' by song playback without viral injections but with laser illumination over HVC (top middle), and 90-day-old pupils that had received optogenetic activation of PAG_{HVC} terminals paired with song playback (bottom middle and bottom). **c**, From left to right, a maximum-projected image of serial sagittal sections of the PAG (left, approximately 0.5 mm lateral of the midline), showing PAG neurons expressing both ChR2 (green) and TH (pseudo-coloured magenta) (arrows), SNc (middle, approximately 0.8 mm lateral of the midline) and VTA (right, approximately 0.3 mm lateral of the midline). Similar results were obtained in six independently repeated experiments. **d**, Multiunit activity in the PAG, showing the time-locked response to laser stimulation at 2 Hz (top) and 20Hz (bottom). **e**, Schematic of optogenetic stimulation of PAG_{HVC} terminals paired with song playback while infusing DA blockers into HVC. **f**, Tutor song similarity of pupils that received activation of PAG_{HVC} terminals paired with song playback while infusing DA blockers into the HVC (red, $n = 3$) was not different from control birds shown in Fig. 3j (Tukey–Kramer test; at 90 days of age; $P = 1.000$), but lower than that received activation of PAG_{HVC} terminals paired with song playback shown in Fig. 3j (Tukey–Kramer test; at 90 days of age; $P = 0.019$). **g**, A sound spectrogram of the song of a 90-day-old pupil that had received optogenetic activation of PAG_{HVC} terminals paired with song playback while infusing DA blockers into the HVC. A sound spectrogram of the song playback used in tutoring sessions is shown in **b**. Data are mean ± s.e.m.

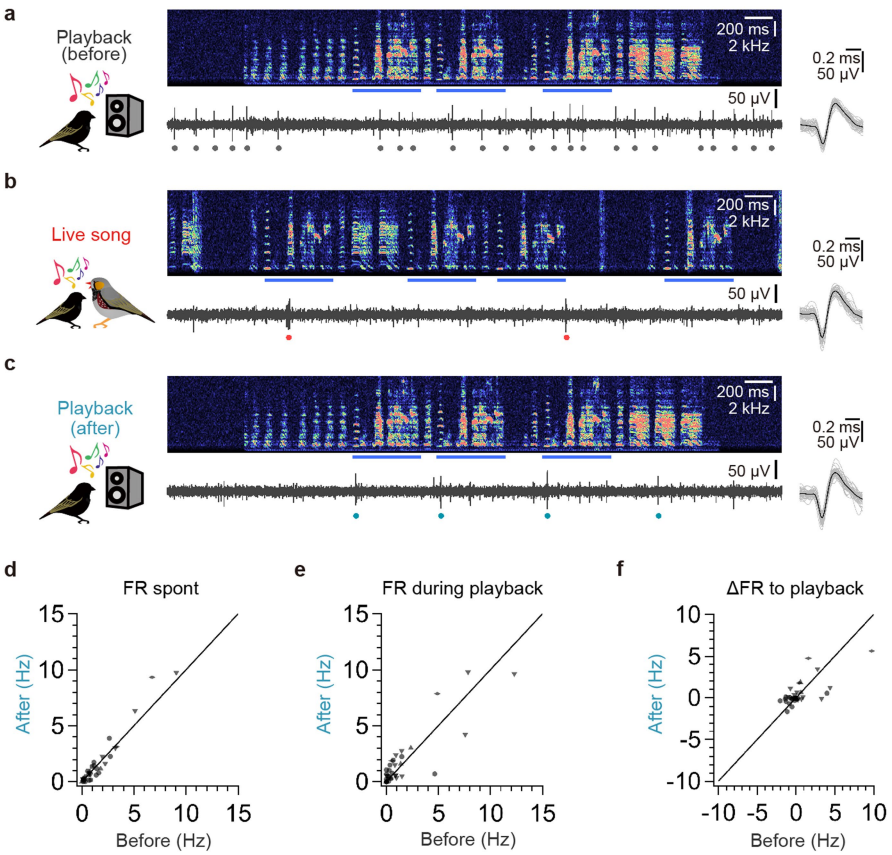

Extended Data Fig. 8 | Action potential activity of HVC neurons in juvenile male zebra finches before and after their first exposure to live tutor songs. a–c, Action potential activity of an HVC neuron to tutor song playback before exposure to a singing tutor (**a**), to live tutor songs (**b**) and to tutor song playback after exposure to live tutor songs (**c**). Top, sound spectrogram. Bottom, voltage recording. Bottom right, 50 action potentials (grey) and their mean (black). Circle, individual action potential; blue bar, tutor song motif. **d**, Spontaneous firing rates (FR spont) of HVC neurons of juvenile males before and after exposure to live tutor songs. Student's two-sided paired *t*-test; mean firing rate before, 1.6 ± 0.3 Hz; mean firing rate after, 1.6 ± 0.4 Hz; $t_{34} = 0.794$, $P = 0.433$, $n = 35$ neurons from four birds. **e**, Firing rates of juvenile male HVC neurons during playback of tutor songs (FR during playback) before and after exposure to live tutor songs. Student's two-sided paired *t*-test; mean firing rate before, 2.0 ± 0.6 Hz; mean firing rate after, 2.1 ± 0.6 Hz; $t_{34} = 0.468$, $P = 0.643$, $n = 35$ neurons from four birds. **f**, Changes in firing rates (ΔFR) of juvenile HVC neurons in response to playback of tutor songs before and after exposure to live tutor songs. Student's two-sided paired *t*-test; ΔFR before, 0.5 ± 0.4 Hz; ΔFR after, 0.5 ± 0.2 Hz; $t_{34} = 0.079$, $P = 0.937$, $n = 35$ neurons from four birds.

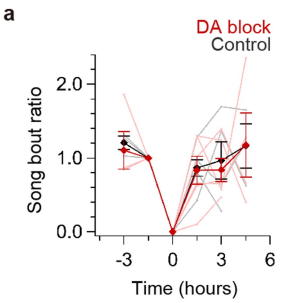

Extended Data Fig. 9 | Song rates of juvenile birds before and after their first tutoring sessions. a, Ratio of song bouts produced before and after the first tutoring session in control birds (black, $n = 6$) and in birds that received an injection of 6-OHDA into the HVC several days before the tutoring session or that were infused with DA blockers into the HVC immediately before and during the tutoring session (red, $n = 6$). Data are mean ± s.e.m.

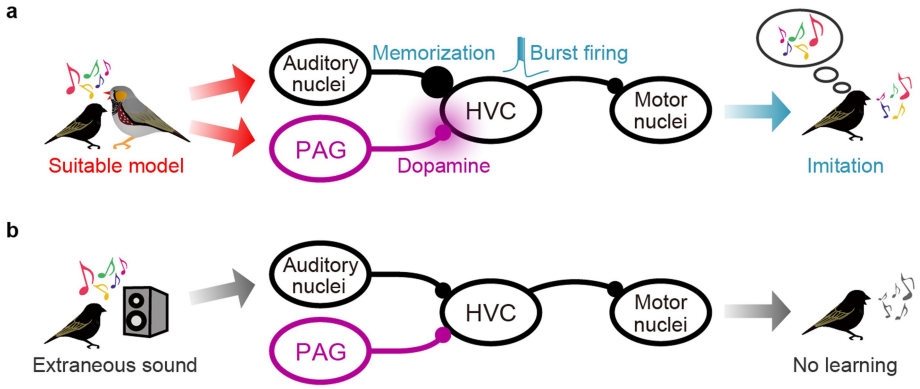

Extended Data Fig. 10 | Summary diagram. a, The presence of a singing tutor (that is, a suitable model) activates auditory afferent neurons and DA-releasing PAG afferent neurons to HVC, leading to potentiation and stabilization of auditory synapses in HVC. This plastic change results in temporally precise coding of the tutor song and increases the occurrence of bursting activity in the HVC, while also rapidly altering temporal and spectral features of the vocalization of a pupil in a manner that drives successful imitation of the tutor song. **b**, Playback of an adult male song without social cues (that is, extraneous sound) only activates auditory afferent neurons in the HVC. The activation of these auditory inputs by itself can neither alter HVC activity nor drive song learning, similar to the condition in which DA signalling in the HVC of the pupil is blocked during the exposure of a juvenile to a live, singing tutor.

nature research

Corresponding author(s): Richard Mooney

Reporting Summary

Nature Research wishes to improve the reproducibility of the work that we publish. This form provides structure for consistency and transparency in reporting. For further information on Nature Research policies, see Authors & Referees and the Editorial Policy Checklist.

Statistical parameters

When statistical analyses are reported, confirm that the following items are present in the relevant location (e.g. figure legend, table legend, main text, or Methods section).

n/a	Confirmed	
☐	☒	The exact sample size (*n*) for each experimental group/condition, given as a discrete number and unit of measurement
☐	☒	An indication of whether measurements were taken from distinct samples or whether the same sample was measured repeatedly
☐	☒	The statistical test(s) used AND whether they are one- or two-sided *Only common tests should be described solely by name; describe more complex techniques in the Methods section.*
☒	☐	A description of all covariates tested
☐	☒	A description of any assumptions or corrections, such as tests of normality and adjustment for multiple comparisons
☐	☒	A full description of the statistics including central tendency (e.g. means) or other basic estimates (e.g. regression coefficient) AND variation (e.g. standard deviation) or associated estimates of uncertainty (e.g. confidence intervals)
☐	☒	For null hypothesis testing, the test statistic (e.g. *F*, *t*, *r*) with confidence intervals, effect sizes, degrees of freedom and *P* value noted *Give P values as exact values whenever suitable.*
☒	☐	For Bayesian analysis, information on the choice of priors and Markov chain Monte Carlo settings
☒	☐	For hierarchical and complex designs, identification of the appropriate level for tests and full reporting of outcomes
☒	☐	Estimates of effect sizes (e.g. Cohen's *d*, Pearson's *r*), indicating how they were calculated
☐	☒	Clearly defined error bars *State explicitly what error bars represent (e.g. SD, SE, CI)*

Our web collection on statistics for biologists may be useful.

Software and code

Policy information about availability of computer code

Data collection	For tetrode recording, RHD2000 Evaluation System Software (intan Technologies, version 1.4) triggered by xpctarget in MATLAB (MathWorks) was used. For sound recording, Sound Analysis Pro 2011 (http://soundanalysispro.com/) was used. For image collection with a confocal microscopy, Las X software (Leica) was used. For image collection with a 2-photon microscopy, MATLAB Scanbox software (Neurolabware) was used.
Data analysis	For calculating tutor song similarity (percent similarity), Sound Analysis Pro 2011 (http://soundanalysispro.com/) was used. For image analysis, ImageJ with Fiji (https://fiji.sc/) was used. For other data analysis and generation of figures, custom function or softwares in Igor Pro (WaveMetrics), MATLAB (MathWorks), C++, and Microsoft Excel were used.

For manuscripts utilizing custom algorithms or software that are central to the research but not yet described in published literature, software must be made available to editors/reviewers upon request. We strongly encourage code deposition in a community repository (e.g. GitHub). See the Nature Research guidelines for submitting code & software for further information.

Data

Policy information about availability of data

All manuscripts must include a data availability statement. This statement should provide the following information, where applicable:

- Accession codes, unique identifiers, or web links for publicly available datasets
- A list of figures that have associated raw data
- A description of any restrictions on data availability

The datasets generated during and/or analysed during the current study are available from the corresponding author on reasonable request.

Field-specific reporting

Please select the best fit for your research. If you are not sure, read the appropriate sections before making your selection.

☒ Life sciences ☐ Behavioural & social sciences ☐ Ecological, evolutionary & environmental sciences

For a reference copy of the document with all sections, see nature.com/authors/policies/ReportingSummary-flat.pdf

Life sciences study design

All studies must disclose on these points even when the disclosure is negative.

Sample size	No sample-size estimation was performed beforehand. Our sample sizes were determined based on sample SD in the earlier sets of experiments, and largely conform to convention in the field.
Data exclusions	Experiments with unsuccessful surgery, injection, implantation, and expression were excluded from the data. Unit activity whose signal-to-noise ratio <3 was excluded from analysis.
Replication	We did our best to use quantified measures such as the cell density and proportion of cells to replicate our findings.
Randomization	Samples were randomly allocated into experimental groups.
Blinding	No blinding was performed. Blinding was difficult in most cases.

Reporting for specific materials, systems and methods

Materials & experimental systems

n/a	Involved in the study
☒	☐ Unique biological materials
☐	☒ Antibodies
☒	☐ Eukaryotic cell lines
☒	☐ Palaeontology
☐	☒ Animals and other organisms
☒	☐ Human research participants

Methods

n/a	Involved in the study
☒	☐ ChIP-seq
☒	☐ Flow cytometry
☒	☐ MRI-based neuroimaging

Antibodies

Antibodies used	Rabbit primary antibody for TH (AB152; MilliporeSigma). Rabbit primary antibody for DBH (22806; ImmunoStar). Anti-rabbit secondary antibody (Jackson ImmunoResearch).
Validation	The primary antibodies have been widely used in rodents. http://www.emdmillipore.com/US/en/product/Anti-Tyrosine-Hydroxylase-Antibody,MM_NF-AB152 http://www.immunostar.com/shop/antibody-catalog/dbh-dopamine-beta-hydroxylase-antibody/ In our study, the antibody for TH labeled large cell bodies in VTA, indicating it labels dopaminergic neurons. In our study, the antibody for DBH labeled many neurons in the locus coeruleus, demonstrating its validity as a marker for noradrenergic neurons.

Animals and other organisms

Policy information about studies involving animals; ARRIVE guidelines recommended for reporting animal research

Laboratory animals	Juvenile male (15-90 d), adult male (> 200 d), and adult female zebra finches (> 200d) (Taeniopygia guttata) raised in the colony were used.
Wild animals	Not used.
Field-collected samples	Not used.